J. Fluid Mech. (1988), *vol.* 186, *pp.* 47–62
Printed in Great Britain

Excitation of instability waves in free shear layers. Part 1. Theory

By D. W. BECHERT

DFVLR, Abteilung Turbulenzforschung, Müller-Breslau-Straße 8, 1000 Berlin-West 12, West Germany

(Received 17 September 1985 and in revised form 20 March 1987)

The generation of instability waves in free shear layers is investigated theoretically. The model assumes an infinitesimally thin shear layer shed from a semi-infinite plate which is exposed to sound excitation. For this model the forced instability waves are calculated. The shear-layer excitation by a source farther away from the plate edge in the downstream direction is very weak while upstream from the plate edge the excitation is relatively efficient. A special solution is given for the source at the plate edge. Any type of source farther away from the plate edge produces a parabolic pressure field near the edge. For this latter, fairly general case, a reference quantity is found for the magnitude of the excited instability waves. The theory is then extended to two streams, one on each side of the shear layer, having different velocities and densities. Furthermore, the excitation of a shear layer in a channel is calculated. The limitations to the theory and some aspects related to experiments are discussed. In particular, for a comparison with measurements, numerical computations of the velocity field outside the shear layer have been carried out.

1. Introduction

In previous investigations it has been shown that the excitation of instability waves in a jet which leads to large-scale structures can enhance the radiated broadband jet noise significantly (Bechert & Pfizenmaier 1975*a*; Moore 1977; Deneuville & Jaques 1977; Schmidt 1978; Hodge & Tam 1981). The excitation of the jet can be produced either by sound or by vorticity convected with the jet flow. The jet shear layer is excited even in such situations where, inadvertently, sound is generated by the apparatus to produce the flow itself (Brown & Roshko 1974; Dziomba & Fiedler 1985; Fiedler & Mensing 1985).

In the case of acoustical excitation of a jet it has also been demonstrated that the production of instability waves in the jet can extract energy from the exciting sound field (Mechel & Ronneberger 1965; Howe 1979, 1980; Bechert 1980; Crighton 1981; Vasudevan, Nelson & Howe 1985). To give an example, at $M = 0.3$ and $kR = 0.1$ (M = jet Mach number, R = nozzle radius and k = acoustic wavenumber) only 1% of the sound power transmitted through the nozzle is found in the radiated far field.

Nevertheless, not much knowledge has been gained on how the magnitude of instability waves is related quantitatively to exterior perturbations. In the present model for this coupling a simplified configuration is considered. A thin semi-infinite shear layer is assumed to be shed from a thin and rigid semi-infinite plate. The shear layer is exposed to acoustical excitation. This simple configuration is tractable mathematically and the analysis provides some insight into the interaction which

would be less readily obtained for a plane or a circular jet. Previous papers, such as those by Orszag & Crow (1970), Crighton & Leppington (1974), Möhring (1975) and Bechert & Michel (1974, 1975) tackled the same issue, but did not produce a sufficient data base for a quantitative comparison with experiments. The present paper may not seem to provide significant theoretical progress, but it does provide this lacking data base. It is a condensed and updated version of a fairly elaborate report (Bechert 1982). Thus, only basic ideas will be outlined and results will be discussed without providing all details of the calculations.

2. One-stream model

Figure 1 shows the simplified configuration which will be modelled mathematically. First, we shall assume that there is no flow above the shear layer. This condition will be relaxed later. The acoustic field is assumed to be produced by a two-dimensional pulsating source outside the shear layer in the fluid at rest. The following simplifying assumptions are introduced: (i) two-dimensional problem; (ii) parallel mean flow; (iii) all fluctuating quantities harmonic in time, i.e. proportional to $e^{-i\omega t}$; (iv) inviscid flow; (v) linearized problem; (vi) incompressible flow; (vii) infinitesimally thin shear layer.

The first five simplifications are common in the stability theory of free jets. The assumption of an inviscid flow works quite well at sufficiently high Reynolds number (Michalke 1965; Freymuth 1966). The linearization is valid for relatively low fluctuation velocities which are found in the interaction region near the end of the splitter plate, as can be concluded from experiments near a nozzle discharge edge (Freymuth 1966; Bechert & Pfizenmaier 1975*b*). The assumption of incompressibility is equivalent to the restriction to small Mach numbers *and* small Helmholtz numbers, where the Helmholtz number is defined as the ratio of the typical length of the problem to the wavelength of the sound waves. For the major part of this paper, small Helmholtz number means that the distance between source and plate edge should be much smaller than the acoustical wavelength. However, if we know the excitation field around the plate edge and our interest is restricted to the evaluation of the shear-layer excitation there, then the relevant length is the interaction region close to the edge. In this latter case, only the interaction region has to be small compared with the acoustical wavelength. It will turn out that this interaction region has a dimension of the order $\bar{U}_0/f$ (where $\bar{U}_0$ is the mean flow velocity and f the sound frequency). Consequently, we should have $\bar{U}_0/f \ll a_0/f$, where a_0/f is the acoustic wavelength. This is equivalent to $M = \bar{U}_0/a_0 \ll 1$, i.e. again the condition of small Mach number. The seventh assumption, the restriction to an infinitesimally thin shear layer will limit the validity range of the theory to the case where the shear-layer thickness is small compared with the wavelength of the instability waves. In other words, the Strouhal number $f\theta/\bar{U}_0$ should be small. θ is the momentum thickness of the shear layer. This latter restriction will be discussed in detail in §5.2.

The classical approach would be to fulfil the boundary conditions at both sides of the shear layer. This means that both the displacement h and the pressure p should be equal there. The displacement h and the velocity v are connected in the following way:

$$v = \frac{\partial h}{\partial t} + \bar{U}\frac{\partial h}{\partial x}. \tag{1}$$

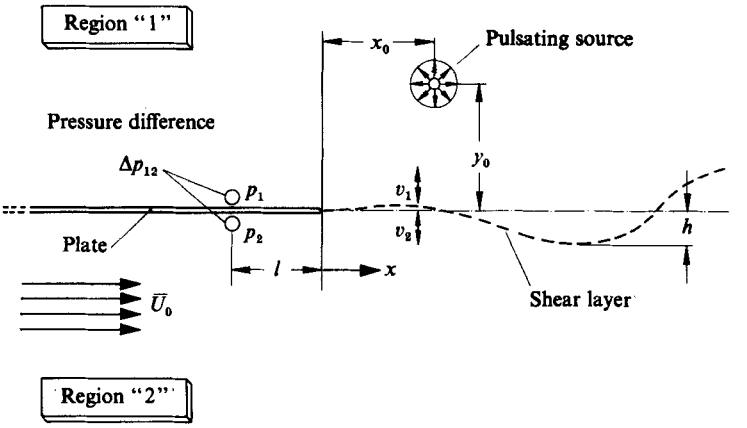

FIGURE 1. Configuration of the analytic model.

For a harmonic motion we find therefore (see also figure 1)

$$v_2 = v_1 + \mathrm{i}\frac{\bar{U}_0}{\omega}\frac{\partial v_1}{\partial x}. \tag{2}$$

This is an equation connecting the v-components of the fluctuation velocities at both sides of the shear layer.

A second equation for v_1 and v_2 will be derived subsequently from a consideration of the pressure field and its gradients at the shear layer. We start out by taking the x-derivative of the first Euler equation and the y-derivative of the second Euler equation. Both derivatives are added and some terms are eliminated using the continuity equation. We end up with

$$\nabla^2 p = -2\rho\frac{\partial v}{\partial x}\frac{\partial \bar{U}}{\partial y}. \tag{3}$$

In our model (see figure 1), the mean velocity profile jumps from $\bar{U} = 0$ for positive y to $\bar{U} = \bar{U}_0$ for negative y. Thus, the right-hand side of (3) exists only *in* the shear layer. Equation (3) can be considered as a non-homogeneous, Laplacean equation with a source distribution of varying strength in the shear layer. It should be stressed here that these sources in the shear layer are pressure sources. Obviously, sources of matter would violate the continuity equation. A discussion on the nature of these sources is given in Bechert (1982, appendix B). The sources in the shear layer consist of a monopole-like contribution which yields a $\delta(y)$-term and a dipole-like contribution which produces a $\delta'(y)$-term. The dipole term becomes negligible for vanishing shear-layer thickness. Thus, the pressure field radiated by the shear layer is symmetrical with respect to y.

At the surface of the semi-infinite plate we have v and $\partial v/\partial x$ equal to zero. Consequently, the pressure source strength is zero on the plate surface. The only other location where $\nabla^2 p$ is non-zero is at the location of the exterior pulsating source (see figure 1).

The basic idea of the present approach is that the pressure distribution in the whole field can be split into two contributions: (i) a pressure field which is *symmetric* with respect to the shear layer and which is caused by the pressure source distribution in the shear layer itself; (ii) a pressure field which is produced by the

exterior forcing, e.g. a pulsating source. The pressure fluctuations of this contribution are transmitted through the shear layer. The pressure gradient of this contribution is continuous through the shear layer and therefore it is *antisymmetric* close to the shear layer.

As a result of this splitting process we have

$$\left.\begin{aligned} p_1 &= p_{1s}+p_{1f}; \quad & p_2 &= p_{2s}+p_{2f}, \\ v_1 &= v_{1s}+v_{1f}; \quad & v_2 &= v_{2s}+v_{2f}. \end{aligned}\right\} \tag{4}$$

The index s stands for shear layer and the index f labels the exterior forcing. The boundary conditions at both sides of the shear layer have to be fulfilled by the summations of the individual constituents, i.e. by v_1 and v_2, as before. On the other hand, we have some new information: since the induced field of the pressure sources in the shear layer is symmetrical (it is created by sources of symmetrical directivity in a field with symmetrical boundary conditions) we obtain

$$\frac{\partial p_{1s}}{\partial y} = -\frac{\partial p_{2s}}{\partial y} \quad \text{at } y = \pm 0 \tag{5}$$

and for the continuous pressure of the exterior forcing

$$\frac{\partial p_{1f}}{\partial y} = \frac{\partial p_{2f}}{\partial y} \quad \text{at } y = \pm 0. \tag{6}$$

These conditions for the pressure gradients in the y-direction can be inserted into the second Euler equation which gives

$$v_{2s} + \mathrm{i}\frac{\bar{U}_0}{\omega}\frac{\partial v_{2s}}{\partial x} = -v_{1s}, \tag{7}$$

$$v_{2f} + \mathrm{i}\frac{\bar{U}_0}{\omega}\frac{\partial v_{2f}}{\partial x} = v_{1f}. \tag{8}$$

Equations (7) and (8) can be added using (4):

$$v_2 + \mathrm{i}\frac{\bar{U}_0}{\omega}\frac{\partial v_2}{\partial x} + v_1 = 2v_{1f}. \tag{9}$$

This is the desired second equation for $v_1$and v_2. The velocity v_{1f} is not an unknown quantity; it is the velocity that is generated by the exterior forcing *without* the mean flow being present, but in the presence of the semi-infinite plate. Equation (2) can be inserted into (9) to obtain the non-homogeneous differential equation

$$2v_1 + 2\mathrm{i}\frac{\bar{U}_0}{\omega}\frac{\mathrm{d}v_1}{\mathrm{d}x} - \left(\frac{\bar{U}_0}{\omega}\right)^2 \frac{\mathrm{d}^2 v_1}{\mathrm{d}x^2} = 2v_{1f}. \tag{10}$$

The complete solution of this type of differential equation is

$$v_1 = C_1 \mathrm{e}^{\lambda_1 x} + C_2 \mathrm{e}^{\lambda_2 x} + \frac{\omega}{\bar{U}_0}\mathrm{e}^{\lambda_2 x}\int_0^x \mathrm{e}^{-\lambda_2 x} v_{1f}\,\mathrm{d}x - \frac{\omega}{\bar{U}_0}\mathrm{e}^{\lambda_1 x}\int_0^x \mathrm{e}^{-\lambda_1 x} v_{1f}\,\mathrm{d}x \tag{11}$$

with the abbreviation

$$\lambda_{1,2} = \frac{\omega}{\bar{U}_0}(\mathrm{i} \pm 1). \tag{12}$$

The first two terms of (11) are the solutions of the homogeneous differential equation. They are identical with the well-known spatial instability waves for an infinitesimally

thin shear layer, extended from $x = -\infty$ to $x = +\infty$, which we shall call the Helmholtz solutions. The constants C_1 and C_2 have the dimension of a velocity and will be determined with the boundary conditions. Equation (11) is a general solution and it has to be evaluated for different excitation velocity distributions v_{1f}. Before doing this, however, we shall discuss the question of the Kutta condition in conjunction with the determination of the constants C_1 and C_2.

2.1. *The Kutta condition*

The following discussion will deal with a fairly general case, where a sound source of any kind is farther away from the trailing edge of the semi-infinite plate. In a previous paper (Bechert & Michel 1975) it has been shown that the induced velocity close to the trailing edge is then

$$v_{1f} = \frac{C_3}{x^{\frac{1}{2}}}, \tag{13}$$

where the coefficient C_3 depends on the strength, location and type of the source. Equation (11) can be evaluated with this distribution

$$v_1 = C_1 e^{\lambda_1 x} + C_2 e^{\lambda_2 x} + C_3 \frac{\omega \pi^{\frac{1}{2}}}{\bar{U}_0}\left(\frac{e^{\lambda_2 x}}{\lambda_2^{\frac{1}{2}}}\operatorname{erf}(\lambda_2 x)^{\frac{1}{2}} - \frac{e^{\lambda_1 x}}{\lambda_1^{\frac{1}{2}}}\operatorname{erf}(\lambda_1 x)^{\frac{1}{2}}\right) \quad \text{for } x \geqslant 0, y = +0. \tag{14}$$

For $x < 0$ we have $v_1 = 0$. Using the condition of equal displacement on both sides of the shear layer, (2), we can also determine v_2.

The two velocity distributions on both sides of the shear layer have to produce equal pressures. We could therefore require equal $\partial p/\partial x$ on both sides. The first Euler equation relates this pressure gradient to the u-velocity component

$$\frac{\partial p}{\partial x} = \rho\left(i\omega u - \bar{U}\frac{\partial u}{\partial x}\right). \tag{15}$$

Consequently, the pressure equilibrium condition can be written in terms of u-velocities:

$$u_1 = u_2 + \frac{i\bar{U}_0}{\omega}\frac{\partial u_2}{\partial x} \quad \text{for } x \geqslant 0. \tag{16}$$

We focus first on the induced u-velocity distribution of the non-homogeneous part of our solution (the term in (14) with coefficient C_3). We can proceed in two different ways: (i) For the non-homogeneous parts of v_1 and v_2 we compute the u-distributions numerically. Exploiting the continuity equation we use a source distribution approach. The numerical data for u_1 and u_2 can be found in Bechert (1982). (ii) We derive a separate differential equation for u_1 similar to that for v_1 (see (10)). The free constants of the u_1 solution are adjusted so that the resulting solution fits to the behaviour of the non-homogeneous part of (14) for large values of x. In this way we obtain an analytical solution for u_1, and, by a similar calculation also one for u_2. The full derivation is given in Bechert (1982). We find

$$u_1 = iC_3\frac{\omega \pi^{\frac{1}{2}}}{\bar{U}_0}\left(\frac{e^{\lambda_1 x}}{\lambda_1^{\frac{1}{2}}} - \frac{e^{\lambda_2 x}}{\lambda_2^{\frac{1}{2}}}\right), \quad u_2 = C_3\frac{\omega \pi^{\frac{1}{2}}}{\bar{U}_0}\left(\frac{e^{\lambda_2 x}}{\lambda_2^{\frac{1}{2}}} + \frac{e^{\lambda_1 x}}{\lambda_1^{\frac{1}{2}}}\right). \tag{17}$$

Both procedures, (i) and (ii), yield the same numerical values. Equations (17) inserted into (16) show pressure equilibrium. Thus, the non-homogeneous part of (14) alone fulfils the conditions of equal displacement and equal pressure at both sides of the shear layer. Consequently, the homogeneous part of the solution has to fulfil the

condition of pressure equilibrium by itself independently. To investigate that, we have to determine the u-velocity field of an instability wave of the type $v \propto e^{\lambda_{1,2}x}$, truncated for $x < 0$. By a source-distribution approach (Bechert 1982) we find u in terms of exponential integrals. After having evaluated these solutions for both sides of the shear layer, we have to insert them into (16) to check the pressure equilibrium. We find that there is no non-zero value of C_1 and C_2 that fulfils (16). Thus, only the non-homogeneous part of (14) is left. As a consequence, the flow leaves the trailing edge tangentially because $v_1 \propto x^{1.5}$ for small x. This is equivalent to a Kutta condition. Thus, mathematically speaking, the Kutta condition is here tied to the symmetry of the pressure field radiated by the shear layer. This symmetry constraint is based on a consideration of the interior of the free shear layer (Bechert 1982, Appendix B). If we relaxed the symmetry constraint, other solutions not fulfilling the Kutta condition could be produced easily (Bechert & Michel 1975; Orszag & Crow 1970).

A complete investigation, however, requires also a discussion of under which circumstances deviations from the Kutta condition may occur. Clearly, our approach will break down for shear layers where the wavelength of the instability waves becomes comparable with the shear-layer thickness. Then, a symmetry argument for the pressure field cannot possibly hold any more. It should be also mentioned that statements on the flow within the shear layer very close to the edge are not possible with our present theoretical approach.

The way in which the Kutta condition starts to fail is clearly exhibited in our previous experiments (Bechert & Pfizenmaier 1975*b*). The envelope $h(x)$ of the shear-layer motion does not everywhere follow the expected behaviour. In particular very close to the trailing edge we find a very small region with a parabolic shape. This is because the convective terms in the equations of motion, which would require a singular behaviour of the fluctuating flow field under these circumstances, are absent in a real flow near a wall. Nevertheless, if one judges from the field shape outside this particular edge region, it still looks as if the Kutta condition is essentially maintained. At high Strouhal numbers, however, this tiny parabolic region near the edge is growing rapidly and it can be assumed that then, and also in the flow outside the shear layer, the Kutta condition is not maintained any more. A more comprehensive discussion of this issue is given in Crighton's (1985) survey paper.

There are other examples of flows where the pressure-symmetry approach is invalid, such as in the wake flows downstream of a cylinder or a plate with a blunt trailing edge. Obviously, these flow configurations are different from ours. In addition, the wavelength of the instability waves that occur is comparable with the wake width. Moreover, wake flows can be absolutely unstable, which means that, for these latter flows, the group speed at a certain frequency becomes zero and temporal wave growth occurs. Or, in other words, the wake flow blows up locally exhibiting one fluctuation frequency which is determined by the flow itself and not by the exterior excitation (Koch 1985; Huerre & Monkewitz 1985; Bechert 1985). The fluctuation magnitude in these latter flows is determined by nonlinear effects and can be changed only by very strong exterior forcing.

On the other hand, there are flows which are convectively unstable. These flows cannot maintain perturbations by themselves. An impulsive excitation causes a perturbation which is swept downstream and dies out eventually at the location of the original excitation. Free shear layers belong to this group (Huerre & Monkewitz 1985; Bechert 1985). The fluctuations exhibited by this class of flows depend on exterior excitation only. In our theory, we predict the excitation for the special case

of a thin shear layer exposed to a fluctuating forcing field, without any claim of further generality. The limits of the validity of this theory are worked out in the second, experimental part of this research (Bechert & Stahl 1988).

2.2. *A reference quantity*

It is of general concern in shear-layer experiments to have a reference quantity for the acoustical excitation. In our above derivation, we have divided the pressure field into two constituents: (i) the pressure field radiated by the shear layer, which is *symmetrical*; and (ii) the pressure field of the excitation which is continuously transmitted through the shear layer and which is *antisymmetrical* close to the shear layer.

Two microphones upstream of the trailing edge and arranged as in figure 1 can be used to isolate the excitation field. If we take the difference of the pressures $p_1 - p_2 = \Delta p_{12}$ we eliminate the symmetrical shear-layer signal completely. By a fairly simple calculation (Bechert 1982) we can also relate the excitation velocity distribution v_{1f} to the pressure difference Δp_{12}:

$$v_{1f} = -\frac{1}{x^{\frac{1}{2}}} \frac{\mathrm{i}\Delta p_{12}}{4\rho\omega l^{\frac{1}{2}}}. \tag{18}$$

In this equation l is the distance between microphones and plate edge (see figure 1). The coefficient i is equivalent to a 90° phase shift. The coefficient C_3 in (17) is also determined by (18). We have, for example, for u_2†

$$u_2 = -\mathrm{i}\frac{\Delta p_{12}}{\rho(\bar{U}_0\omega l)^{\frac{1}{2}}} \frac{1}{4}\pi^{\frac{1}{2}} \left(\frac{\mathrm{e}^{\lambda_2 x}}{(\mathrm{i}-1)^{\frac{1}{2}}} + \frac{\mathrm{e}^{\lambda_1 x}}{(\mathrm{i}+1)^{\frac{1}{2}}} \right). \tag{19}$$

If we are mainly interested in the modulus of u_2 for distances slightly downstream of the plate edge where the decaying wave has vanished, we find

$$|u_2| = \frac{|\Delta p_{12}|}{\rho(\bar{U}_0\omega l)^{\frac{1}{2}}} \frac{\pi^{\frac{1}{2}}}{4\times 2^{\frac{1}{4}}} \mathrm{e}^{\omega x/\bar{U}_0} \quad \text{for } x > \frac{\bar{U}_0}{f}. \tag{20}$$

We shall verify this equation experimentally in order to test the present theory. In the experiments we can use $\Delta p_{12}/l^{\frac{1}{2}}$ as a reference quantity because it does not depend on the mean flow conditions, or we non-dimensionalize the fluctuating velocity in the following way:

$$\tilde{u}_2 = u_2 \frac{\rho(\bar{U}_0\omega l)^{\frac{1}{2}}}{\Delta p_{12}}. \tag{21}$$

It is also convenient to non-dimensionalize the downstream distance x

$$\tilde{x} = \frac{x\omega}{\bar{U}_0}. \tag{22}$$

So we obtain for (20)

$$|\tilde{u}_2| = \frac{\pi^{\frac{1}{2}}}{4\times 2^{\frac{1}{4}}} e^{\tilde{x}}. \tag{23}$$

2.3. *The u-velocity field*

The fluctuating quantity that can be measured most easily and accurately is the velocity u_2 in the flow region ($y < 0$, see figure 1). This is the reason why this particular quantity has been computed numerically. A source-distribution approach

† Unfortunately, this equation has been mistyped in Bechert (1982).

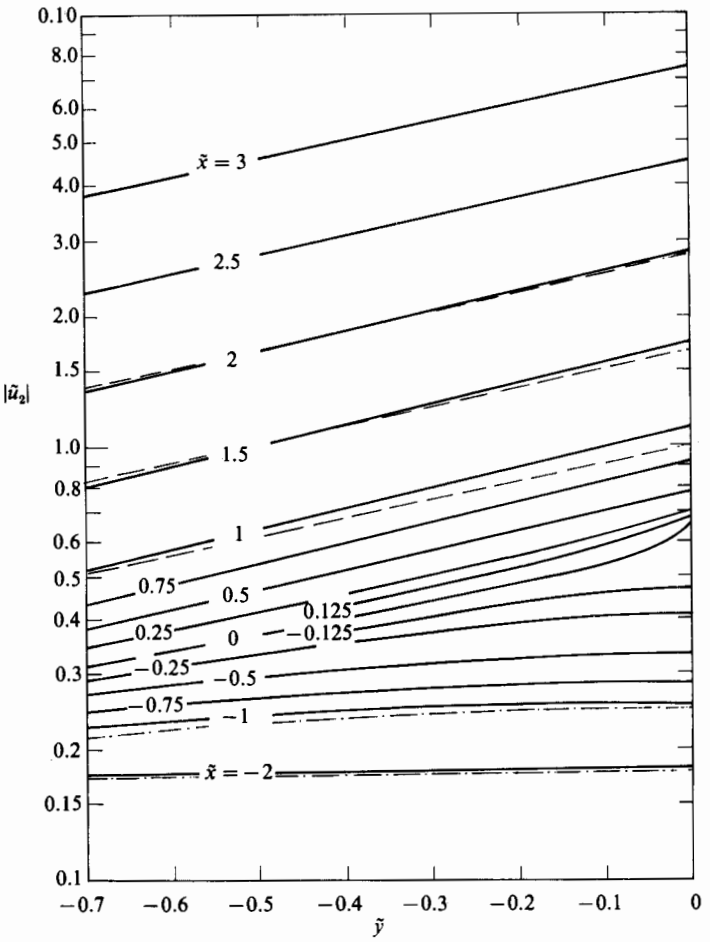

FIGURE 2. Computed distribution of $|\tilde{u}_2|$ for various $\tilde{x}$ and $\tilde{y}$: ---, downstream amplified instability wave alone; —·—, acoustic excitation alone.

is used to compute u_2 from v_2 at $y = -0$. v_2 is given analytically for all x. In figure 2 the computed curves of the modulus of u_2 are plotted in non-dimensionalized form versus $\tilde{y} = y\omega/\bar{U}_0$ for different downstream distances $\tilde{x} = x\omega/\bar{U}_0$ from the plate edge. The vertical scaling in figure 2 is logarithmical. Therefore, an exponential curve appears as a straight line. Such straight lines are found for locations farther downstream of the edge. At $\tilde{x} = 2$, for example, which corresponds to $\frac{1}{3}$ wavelength of the instability waves, the induced field is already dominated by the amplified instability wave. On the other hand, upstream of the edge at $\tilde{x} = -2$, the u-fluctuation is governed by the acoustic excitation field alone. For these two regions we also find fairly simple asymptotic equations (see Bechert 1982).

3. Two streams with different densities

The condition of equal displacements on both sides of the shear layer is also valid in this more general case. For the pressure we have the same conditions as before, i.e. we have $\nabla^2 p = 0$ outside the shear layer and outside the location of the sound source. In addition, the pressure has to be the same on both sides of the shear layer. For

equal boundary conditions above and below the shear layer we can use the previous approach using the symmetry and antisymmetry of pressure gradients. Consequently, the structure of the solutions will be similar to the one-stream model considered in §2. However, the mathematics is much more tedious. The details are given in Bechert (1982).

The equation for u_2 corresponding to (19) for the one-stream case reads:

$$u_{2_{(y=-0)}} = -\mathrm{i}\frac{\Delta p_{12}}{\rho_2(\bar{U}_2\omega l)^{\frac{1}{2}}}\tfrac{1}{4}\pi^{\frac{1}{2}}\frac{1}{\left(1+\dfrac{\rho_1\bar{U}_1^2}{\rho_2\bar{U}_2^2}\right)}\left[\frac{1+\mathrm{i}\dfrac{\bar{U}_1}{\bar{U}_2}\left(\dfrac{\rho_1}{\rho_2}\right)^{\frac{1}{2}}}{\tilde{\lambda}_1^{\frac{1}{2}}}\mathrm{e}^{\tilde{\lambda}_1\tilde{x}}+\frac{1-\mathrm{i}\dfrac{\bar{U}_1}{\bar{U}_2}\left(\dfrac{\rho_1}{\rho_2}\right)^{\frac{1}{2}}}{\tilde{\lambda}_2^{\frac{1}{2}}}\mathrm{e}^{\tilde{\lambda}_2\tilde{x}}\right], \tag{24}$$

with

$$\tilde{\lambda}_{1,2} = \frac{1}{1+\dfrac{\rho_1\bar{U}_1^2}{\rho_2\bar{U}_2^2}}\left[\mathrm{i}\left(1+\frac{\rho_1\bar{U}_1}{\rho_2\bar{U}_2}\right)\pm\left(1-\frac{\bar{U}_1}{\bar{U}_2}\right)\left(\frac{\rho_1}{\rho_2}\right)^{\frac{1}{2}}\right] \tag{25}$$

and $\tilde{x} = \omega x/\bar{U}_2$. In these equations $\bar{U}_1$, ρ_1 are mean flow velocity and density above the shear layer and $\bar{U}_2$, ρ_2 are the same quantities below the shear layer. We assume that $\bar{U}_2 > \bar{U}_1$; u_2 is the fluctuation velocity just below the shear layer. All other quantities are defined as before. For $\omega x/\bar{U}_2 > 1$, where the decaying instability wave becomes unimportant, we obtain a somewhat simplified equation for the modulus of u_2:

$$|u_2|_{(y=-0)} = \frac{|\Delta p_{12}|}{\rho_2(\bar{U}_2\omega l)^{\frac{1}{2}}}\tfrac{1}{4}\pi^{\frac{1}{2}}\frac{\exp\left[(1-\bar{U}_1/\bar{U}_2)(\rho_1/\rho_2)^{\frac{1}{2}}\omega x/\bar{U}_2\right]}{(\rho_1/\rho_2)^{\frac{1}{2}}[(1+\rho_1/\rho_2)(1+\rho_1\bar{U}_1^2/\rho_2^2\bar{U}_2^2)]^{\frac{1}{4}}}. \tag{26}$$

We find a decreased amplification rate in the downstream direction if the density of the faster stream is higher and if the velocity difference between the two streams decreases. The susceptibility of the shear layer is also changed, but less dramatically (see the denominator of (26)), with changing velocities and densities. However, if we have such strong differences in density as between air and water then also jet amplification and sensitivity will change very significantly.

For comparison with the experiments in the second part of this paper (Bechert & Stahl 1988) we consider also the particular case with $\rho_1 = \rho_2 = \rho$ and $\bar{U}_1 = 0.1\bar{U}_2$. Taking the modulus of u_2 from (24), we obtain after some intermediate calculations

$$|u_2|_{(y=-0)} = \frac{|\Delta p_{12}|}{\rho(\bar{U}_2\omega l)^{\frac{1}{2}}}0.372\,(\mathrm{e}^{1.8\omega x/\bar{U}_2}+\mathrm{e}^{-1.8\omega x/\bar{U}_2}+1.266)^{\frac{1}{2}}. \tag{27}$$

4. The relative importance of the edge region

In this and the following sections we confine our considerations again to the one-stream case with no flow above the shear layer. There is no particular difficulty, however, to extend all following considerations to the case of having a different stream on each side of the shear layer. In §2.2 it had been mentioned that under almost all conceivable circumstances, a parabolic pressure field is produced close to the plate edge. The relevance of this region to the shear layer excitation will be shown with a simple model (see figure 3). The shear-layer velocity v_1 far downstream of the edge will be determined if a pulsating (two-dimensional) monopole source is located at different positions: (*a*) close to the shear layer, (*b*) above the edge or (*c*) upstream of the edge (see figure 3). In the following calculation we shall only consider the

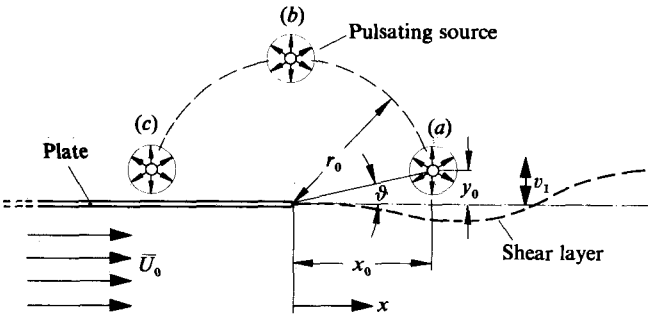

FIGURE 3. Shear-layer excitation by a monopole source.

amplified instability wave constituent and not the decaying one, because this is irrelevant at great distances $x \gg \bar{U}_0/\omega$. We have from (11) with $C_1 = C_2 = 0$:

$$v_1 = -\frac{\omega}{\bar{U}_0} e^{\lambda_1 x} \int_0^\infty e^{-\lambda_1 x} v_{1f}\, dx \quad \text{for } x \gg \frac{U_0}{\omega} \tag{28}$$

with

$$\lambda_1 = \frac{\omega}{\bar{U}_0}(i+1).$$

If the upper boundary of the integral in (11) is set equal to infinity, like in (28), the total influence of the excitation is included. This expansion will provide the magnitude of the instability wave downstream of the interaction region with the monopole field. Bechert & Michel (1975) give the induced field of a monopole above a semi-infinite plate. We have for v_{1f}

$$v_{1f} = -\frac{Q}{4\pi}(2(r_0 - x_0))^{\frac{1}{2}} \frac{1}{x^{\frac{1}{2}}} \frac{x + r_0}{[(x-x_0)^2 + y_0^2]}, \tag{29}$$

with $r_0^2 = x_0^2 + y_0^2$ and Q being the source strength $Q = Q_0 e^{-i\omega t}$. The last term of (29) can be split into two parts

$$\frac{x + r_0}{(x-x_0)^2 + y_0^2} = \frac{1}{2}\left[\frac{\bar{T}}{x - z_0} + \frac{T}{x - \bar{z}_0}\right], \tag{30}$$

with

$$\left.\begin{aligned} z_0 &= x_0 + iy_0; \quad \bar{z}_0 = x_0 - iy_0; \\ T &= 1 + \frac{i(r_0 + x_0)}{y_0}; \quad \bar{T} = 1 - \frac{i(r_0 + x_0)}{y_0}. \end{aligned}\right\} \tag{31}$$

We are left with integrals of the type

$$\int_0^\infty \frac{e^{-\lambda_1 x}\, dx}{x^{\frac{1}{2}}(x+\tau)} = \frac{\pi}{\tau^{\frac{1}{2}}} e^{\tau\lambda_1} \operatorname{erfc}(\tau\lambda_1)^{\frac{1}{2}}. \tag{32}$$

The solution of the integral in (32) can be found in tables for Laplace transforms or in Abramovitz & Stegun (1970). We end up with the following analytic solution†

$$v_1 = +\frac{Q\omega(2(r_0 - x_0))^{\frac{1}{2}}}{8\bar{U}_0} e^{\lambda_1 x}\left[\frac{\bar{T}}{-z_0^{\frac{1}{2}}} e^{-z_0\lambda_1} \operatorname{erfc}(-z_0\lambda_1)^{\frac{1}{2}} + \frac{T}{-\bar{z}_0^{\frac{1}{2}}} e^{-\bar{z}_0\lambda_1} \operatorname{erfc}(-\bar{z}_0\lambda_1)^{\frac{1}{2}}\right]. \tag{33}$$

† This solution differs by the coefficient $\frac{1}{2}$ from a solution given previously (Bechert & Michel 1975), where this coefficient had been omitted erroneously.

The solution contains x only in the instability-wave term $e^{\lambda_1 x}$, but the coefficient governing the magnitude of these waves is fairly complex. We shall, therefore, expand the solution for two typical cases, i.e. an excitation by a monopole source farther away from the lip ($r_0\omega/\bar{U} \gg 1$) and an excitation directly at the lip of the semi-infinite plate.

For the excitation at large distances, we have to expand the complex error functions for large arguments. If we take only the first term of the series expansion, we find after some intermediate calculations for the modulus of v_1:

$$|v_1| = \frac{Q_0}{2\pi r_0^{\frac{1}{2}}} \sin\tfrac{1}{2}\vartheta \left(\frac{\omega}{\bar{U}_0}\right)^{\frac{1}{2}} \frac{\pi^{\frac{1}{2}}}{2^{\frac{1}{4}}} e^{\omega x/\bar{U}_0} \left[1 + \frac{\bar{U}_0}{2\omega r_0}(\cos\vartheta + \tfrac{1}{2}\cos 2\vartheta)\right] \quad \text{for } \frac{\omega r_0}{\bar{U}_0} \gg 1, \quad x \gg r_0. \tag{34}$$

The first part of this equation closely resembles the excitation velocity in the neighbourhood of the plate edge

$$v_{1f} = -\frac{Q}{2\pi r_0^{\frac{1}{2}}} \sin\tfrac{1}{2}\vartheta \frac{1}{x^{\frac{1}{2}}} \quad \text{for } x \ll r_0. \tag{35}$$

One would obtain the following expression:

$$|v_1| = \frac{Q_0}{2\pi r_0^{\frac{1}{2}}} \sin\tfrac{1}{2}\vartheta \left(\frac{\omega}{\bar{U}_0}\right)^{\frac{1}{2}} \frac{\pi^{\frac{1}{2}}}{2^{\frac{1}{4}}} e^{\omega x/\bar{U}_0} \quad \text{for } \frac{\omega x}{\bar{U}_0} \gg 1 \tag{36}$$

if one calculated the excitation by the parabolic field at the plate edge, (35), alone. Therefore, the expression in brackets in (34) reflects the additional interaction with the source field farther downstream of the plate edge. The deviations from the pure interaction at the plate edge become small if $\omega r_0/\bar{U}_0 > 1$. The conclusion from this is that the parabolic field at the plate edge dominates if the source is farther away from the edge. Consider the situation shown in figure 3. In which location (*a*), (*b*) or (*c*) of the source will the interaction be the strongest? Equation (34) will give a clear answer: at (*c*), upstream of the shear layer!

In that context an interesting question is how far an 'exterior excitation' can come from the turbulent shear layer itself downstream of the plate edge in a real flow situation. In our model, the pressure sources of the shear-layer motion lie in the $y = 0$-plane. Therefore, in this model, no feedback from the downstream perturbations is possible ($\sin\frac{1}{2}\vartheta = 0$). However, in a real situation $\nabla^2 p = 0$ is still valid outside the shear layer. The pressure sources are in a region of small ϑ. Therefore, a very weak feedback of the downstream turbulent flow is possible. This consideration is not as naïve as it seems at first glance, because the equation $\nabla^2 p = -2\rho(\partial\bar{U}/\partial y)(\partial v/\partial x)$ is also valid in three dimensions. The source term on the right-hand side might look slightly different in a nonlinear flow situation, but the concept of having linearly superposable pressure sources in the shear layer will not break down, because the pressure is a linear quantity in all our equations, and deviations of this linearity will occur only if the pressure perturbation is of the same order as the ambient gas pressure. Anyway, (34) shows clearly why shear layers are highly sensitive to perturbations (such as sound) coming from upstream and not very sensitive to perturbations having their origin downstream of the edge in the shear layer.

Those who are familiar with experiments on excited jets know that an excitation close to the lip is very efficient. The preceding calculations did not consider this case

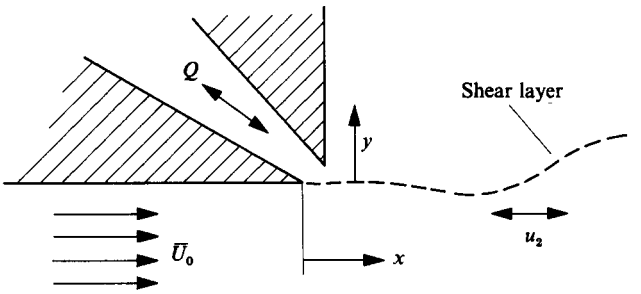

FIGURE 4. Real edge excitation configuration.

because it was assumed that $\omega r_0/\bar{U}_0 \gg 1$. On the other hand, (33) can be also expanded for $\omega r_0/\bar{U}_0 \ll 1$, which would include the lip-excitation case.

After some intermediate calculations we find

$$v_1 = \frac{Q\omega}{2\bar{U}_0} e^{\lambda_1 x}\left[e^{-x_0\lambda_1}\cos(y_0\lambda_1) - 2\left(\frac{r_0\lambda_1}{\pi}\right)^{\frac{1}{2}}\sin\tfrac{1}{2}\vartheta\right], \tag{37}$$

with

$$\lambda_1 = \frac{\omega}{\bar{U}_0}(i+1)$$

and valid for $\omega r_0/\bar{U}_0 \ll 1$ and $\omega x/\bar{U}_0 \gg 1$.

There is some interesting physics hidden in (37). Assume that $|y_0\lambda_1| \to +0$ and $(r_0\lambda_1)^{\frac{1}{2}}\sin\frac{1}{2}\vartheta \to 0$. Then we have a source just above the shear layer at positive x_0. The source acts then as a δ-function with strength $\frac{1}{2}Q$ on the shear layer. $\frac{1}{2}Q$ is just the flux which penetrates through the shear-layer plane. With this in mind we reconsider the general solution for the shear-layer motion, (11), with $C_1 = C_2 = 0$. For v_{1f} we have

$$v_{1f} = -\tfrac{1}{2}Q\,\delta(x-x_0) \quad \text{at } y = +0. \tag{38}$$

With (11) we find the complete solution at once:

$$v_1 = \frac{Q\omega}{2\bar{U}_0}[e^{\lambda_1 x}e^{-\lambda_1 x_0} - e^{\lambda_2 x}e^{-\lambda_2 x_0}]. \tag{39}$$

For the pure lip excitation with $|\lambda_1 x_0| \to 0$ we have a simple analytic solution which might be utilized if the free shear layer is excited just at the plate edge

$$v_1 = \frac{Q\omega}{2\bar{U}_0}(e^{\lambda_1 x} - e^{\lambda_2 x}). \tag{40}$$

Also the u-distribution in the whole ambient field can be written in closed form. It contains exponential integrals of complex argument for the induced field of the instability waves truncated at $x = 0$ ($v_1 = 0$ for $x < 0$) and the induced field of the source (see Bechert & Michel 1974; Bechert 1982). For distances farther downstream, we have an extremely simple equation for the magnitude of the instability waves, where $|v_1| = |v_2| = |u_1| = |u_2|$. We find

$$|u_2| = \frac{Q\omega}{2\bar{U}_0} e^{\omega x/\bar{U}_0} \quad \text{at } y = -0 \tag{41}$$

and with the introduction of the decay in the y-direction

$$|u_{1,2}| = \frac{Q\omega}{2\bar{U}_0} e^{\omega(x-|y|)/\bar{U}_0} \quad \text{for } x > \frac{\bar{U}_0}{\omega}, \quad y \neq 0. \tag{42}$$

Q is the volume flux (say, in m^2/s) of the excitation source. In a real situation with an arrangement like the one shown in figure 4 we suspect that more than half of the volume flux Q penetrates through the $y = 0$ plane. Therefore, the efficiency might be even slightly higher than suggested by (42).

5. Theory pertaining to the experiments

This section deals with theoretical problems arising from an experiment which inevitably cannot be carried out under completely ideal conditions. One such deviation is the presence of additional walls in a typical experiment with a shear layer in the middle of a rectangular channel. Another limitation to the validation of our theory is the presence of a shear layer of finite thickness in a real experiment.

5.1. *Shear layer in a channel*

It is not possible to produce an infinitely wide stream in an experiment. Therefore, we have to investigate what the influence of the finite dimensions of an experimental set-up might be. A typical configuration is a shear layer in the centreline of a channel with rectangular cross-section. Owing to the presence of the additional channel walls on both sides of the shear layer we will find certain deviations. A detailed investigation (Bechert 1982) has shown that in particular the excitation field is changed. Instead of having $v_{1f} \propto 1/x^{\frac{1}{2}}$ (see (18)), we find by virtue of conformal mapping

$$v_{1f} = -\frac{(\pi/d)^{\frac{1}{2}}}{(e^{\pi x/d}-1)^{\frac{1}{2}}}\frac{i\Delta p_{12}}{4\rho\omega l^{\frac{1}{2}}}, \tag{43}$$

where d is the half-width of the channel. This means that close to the plate edge the excitation is still parabolic and proportional to $1/x^{\frac{1}{2}}$, whereas farther downstream it decays exponentially. The new excitation field can be inserted into the general solution, (11). Downstream of the interaction region at the plate edge one can calculate an analytic solution which contains gamma functions of complex argument (Bechert 1982). However, we can find a much simpler solution for the practically important case where the wavelength of the instability waves is much smaller than the channel half-width d. In this case we obtain by an expansion of the analytic solution

$$|u_2| = \frac{|\Delta p_{12}|}{\rho(\bar{U}_0\omega l)^{\frac{1}{2}}}\frac{\pi^{\frac{1}{2}}}{4\times 2^{\frac{1}{4}}}e^{\omega x/\bar{U}_0}\left(1-\tfrac{1}{16}\pi\frac{\bar{U}_0}{\omega d}\right). \tag{44}$$

The last term in brackets of this equation reflects the influence of the presence of the walls. The theory also provides a simple analytic solution for the case when the two microphones sensing Δp_{12} are moved upstream to a location where the pressure field is not parabolic any more due to the influence of the channel walls. In this case the quantity $l^{\frac{1}{2}}$ in (43) and (44) has to be replaced by the expression:

$$l^{\frac{1}{2}} \rightarrow \frac{d^{\frac{1}{2}}}{2\pi^{\frac{1}{2}}}\ln\left[\frac{1+(1-e^{-\pi l/d})^{\frac{1}{2}}}{1-(1-e^{-\pi l/d})^{\frac{1}{2}}}\right]. \tag{45}$$

The detailed calculations leading to this result are given in Bechert (1982).

5.2. *Finite shear-layer thickness effects*

There is not yet any direct way to test the limits of our mathematical model if we consider the validity range towards increasing frequencies (or Strouhal numbers).

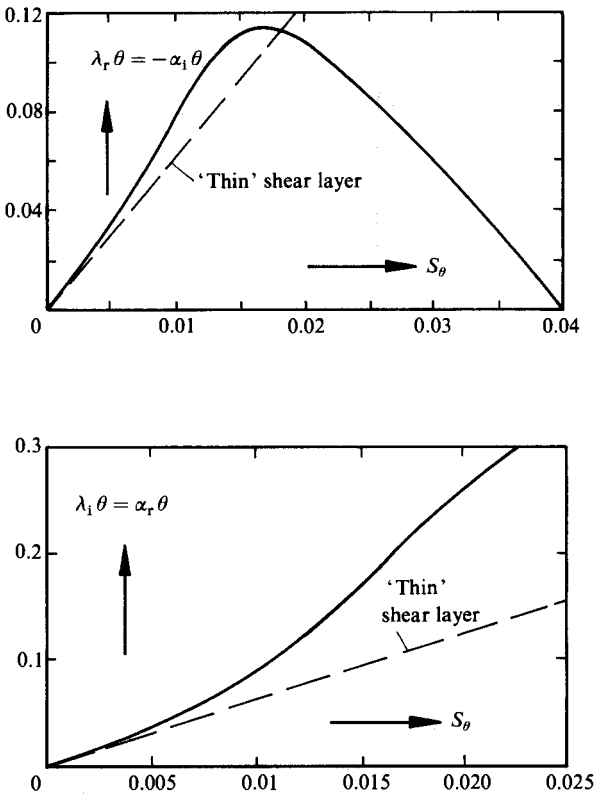

FIGURE 5. Amplification rate ($\lambda_r\theta$) and wavenumber ($\lambda_i\theta$) of a shear layer with finite thickness, according to Michalke (1965).

However, if we compare our case to a shear layer extending from $x = -\infty$ to $x = +\infty$, we can utilize the results of conventional stability theory to estimate where our approach becomes invalid. From previous work (Michalke 1965; Freymuth 1966) it can be concluded that wavenumber and downstream amplification rate of (infinitely extended) shear layers of finite thickness deviate with increasing Strouhal numbers S_θ from the predicted values for an infinitesimally thin shear layer. The amplification rate and the phase speed, according to Michalke (1965) are given in figure 5.

The data in figure 5 refer to a hyperbolic tangent mean velocity profile. It can be seen that for increasing S_θ the deviations in the wavenumber are much more significant than for the amplification rate. An increased wavenumber also causes an enhanced decay of the induced velocity field in the y-direction.

For further sophistication, the combined influence of entrainment and finite shear-layer thickness can also be taken into account, using the work of Monkewitz & Huerre (1982), where computations are given for a shear layer between two streams of different velocities.

The present work has been sponsored partly by NASA Lewis (Contract NAG 3-198) and by the Deutsche Forschungsgemeinschaft (Contract Be 889/1 – 1). The field calculations in §2.3 are a repetition of earlier computations carried out by Dr M. Nallasamy (University of Houston). The author was encouraged by Professor A. K.

M. F. Hussain (University of Houston) to carry out this research. He arranged also for the author's visit to Houston in this joint U.H.–DFVLR project. The author is also indebted to Dr W. F. King, DFVLR Berlin, for a careful review of this paper. The author appreciates also the advice of Professor N. Nullschnall and Dr N. Nörgel who helped to establish this paper in the present form.

REFERENCES

ABRAMOVITZ, M. & STEGUN, I. A. (Ed.) 1970 *Handbook of Mathematical Functions*. Dover.

BECHERT, D. W. 1980 Sound absorption caused by vorticity shedding, demonstrated with a jet flow. *J. Sound Vib.* **70**, 389–405.

BECHERT, D. W. 1982 Excited waves in shear layers. *DFVLR-FB* 82–23.

BECHERT, D. W. 1985 Excitation of instability waves. *Z. Flugwiss. Weltraumforsch.* **9**, 356–361.

BECHERT, D. W. & MICHEL, U. 1974 The control of a thin free shear layer with and without a semi-infinite plate with a pulsating monopole or dipole. Some new closed form solutions. *DFVLR-FB* 74-22.

BECHERT, D. W. & MICHEL, U. 1975 The control of a thin free shear layer with and without a semi-infinite plate by a pulsating flow field. *Acustica* **33**, 287–307.

BECHERT, D. W. & PFIZENMAIER, E. 1975*a* On the amplification of broad band jet noise by a pure tone excitation. *J. Sound Vib.* **43**, 581–587.

BECHERT, D. W. & PFIZENMAIER, E. 1975*b* Optical compensation meaurements on the unsteady exit condition at a nozzle discharge edge. *J. Fluid Mech.* **71**, 123–144.

BECHERT, D. W. & STAHL, B. 1988 Excitation of instability waves in free shear layers. Part 2. Experiments. *J. Fluid Mech.* **186**, 63–84.

BROWN, G. L. & ROSHKO, A. 1974 On density effects and large structure in turbulent mixing layers. *J. Fluid Mech.* **64**, 775–816.

CRIGHTON, D. G. 1981 Acoustics as a branch of fluid mechanics. *J. Fluid Mech.* **106**, 261–298.

CRIGHTON, D. G. 1985 The Kutta condition in unsteady flow. *Ann. Rev. Fluid Mech.* **17**, 411–445.

CRIGHTON, D. G. & LEPPINGTON, F. G. 1974 Radiation properties of the semi-infinite vortex sheet: the initial value problem. *J. Fluid Mech.* **64**, 393–414.

CROW, S. C. & CHAMPAGNE, F. H. 1971 Orderly structure in jet turbulence. *J. Fluid Mech.* **48**, 547–591.

DENEUVILLE, P. & JAQUES, J. 1977 Jet noise amplification: a practically important problem. *AIAA paper* 77-1368.

DZIOMBA, B. & FIEDLER, H. E. 1985 Effect of initial conditions on two-dimensional free shear layers. *J. Fluid Mech.* **152**, 419–442.

FIEDLER, H. E. & MENSING, P. 1985 The plane turbulent shear layer with periodic excitation. *J. Fluid Mech.* **150**, 281–309.

FREYMUTH, P. 1966 On transition in a separated laminar boundary layer. *J. Fluid Mech.* **25**, 683–703.

HODGE, C. G. & TAM, C. K. W. 1981 In *Aerospace Highlights 1981. Astronautics and Aeronautics, Dec. 1981*, pp. 28–29.

HOWE, M. S. 1979 Attenuation of sound in a low Mach number nozzle flow. *J. Fluid Mech.* **91**, 209–229.

HOWE, M. S. 1980 The dissipation of sound at an edge. *J. Sound Vib.* **70**, 407–411.

HUERRE, P. & MONKEWITZ, P. A. 1985 Absolute and convective instabilities in free shear layers. *J. Fluid Mech.* **159**, 151–168.

KOCH, W. 1985 Local instability characteristics and frequency determination of self-excited wake flows. *J. Sound Vib.* **99**, 53–83.

MECHEL, F. & RONNEBERGER, D. 1965 Experimentelle Untersuchung der Schallausbreitung in luftdurchströmten Rohren mit Querschnittsveränderungen (Experimental investigation on the sound propagation in tubes with air flow and with changes in cross section). *5th Intl Congr. on Acoustics, Liège, 1965, paper* K 23.

MICHALKE, A. 1965 On spatially growing disturbances in an inviscid shear layer. *J. Fluid Mech.* **23**, 521–544.

MÖHRING, W. 1975 On flows with vortex sheets and solid plates. *J. Sound Vib.* **38**, 403–412.

MONKEWITZ, P. A. & HUERRE, P. 1982 Influence of the velocity ratio on the spatial instability of mixing layers. *Phys. Fluids* **25**, 1137–1143.

MOORE, C. J. 1977 The role of shear-layer instability waves in jet exhaust noise. *J. Fluid Mech.* **80**, 321–367.

ORSZAG, S. A. & CROW, S. C. 1970 Instability of a vortex sheet, leaving a semi-infinite plate. *Stud. Appl. Maths* **49**, 167–181.

SCHMIDT, C. 1978 Aerodynamic characterization of excited jets. *J. Sound Vib.* **61**, 148–152.

VASUDEVAN, M. S., NELSON, P. A. & HOWE, M. S. 1985 An experimental study of the influence of mean flow on acoustic dissipation by vorticity production at edges. *Aero- and Hydro-Acoustics, IUTAM Symp. Lyon.* Springer-Verlag.